Table 1 Storage needs and operation counts

Algorithm:	BTDMIA		Present	
Bordering:	Without	With	Without	With
(loc)	$n(\mu'+n)$	When $k>k'$ add:	$n\mu$	When $k>k'$ add:
(mul, add)	$n(\mu\mu'-\ell^2)$	$n\,(k-k')\,(n-m)$	$n(\mu\mu'-\ell^2)$	$n\,(k-k')\,(n-m)$
(sol)	μ	$k-k'$	μ	
LOOPs	2	3	2	3

To assess the present algorithm as compared with the BTDMIA, we give, in Table 1, their storage needs and operation counts per grid point, when both are applied, without and with bordering, to the inverse boundary-layer problem described earlier. For fair comparison when $m > m'$, the two methods should operate in opposite directions. The forward sweep of the present algorithm is to be carried out starting from the side with m conditions, whereas its counterpart of the most efficient form[5] of the BTDMIA is to be carried out starting from the other side.

The conclusion is twofold: non-bordering is superior to bordering. The present algorithm is more efficient than the BTDMIA.

References

[1]Bradshaw, P., Cebeci, T., and Whitelaw, J. H., *Engineering Calculation Methods for Turbulent Flows*, Academic Press, New York, 1981.

[2]Chen, H. H., and Cebeci, T., "Bordering Algorithm for Solution of Boundary-Layer Equations in Inverse Mode," *AIAA Journal*, Vol. 29, No. 12, 1991, pp. 2257–2259.

[3]Cebeci, T., Keller, H. B., and Williams, P. G., "Separating Boundary-Layer Flow Calculations," *Journal of Computational Physics*, Vol. 31, 1979, pp. 363–378.

[4]Wornom, S. F., "A Fourth-Order Box Method for Solving the Boundary-Layer Equations," NASA TM X-74000, Jan. 1977.

[5]Keller, H. B., "Accurate Difference Methods for Nonlinear Two-Point Boundary Value Problems," *SIAM Journal of Numerical Analysis*, Vol. 11, No. 2, 1974, pp. 305–320.

Derivation of a Modified Hybrid Approximation

Thomas M. Harms,* Theodor W. von Backström,†
J. Prieur du Plessis,‡ and Louwrens M. Toerien§
University of Stellenbosch, Stellenbosch 7600, South Africa

I. Introduction

CONTROL volume interface interpolation schemes can be classified as to whether they are local grid- or streamline orientated and whether they are algebraically or physically based. The hybrid scheme described by Spalding[1] is an example of a grid-line-orientated physically based scheme. The exponential coefficient function resulting from the analytic solution of a one-dimensional homogeneous convection-diffusion equation, i.e.,

$$A(Pe) = Pe/(e^{Pe}-1) \tag{1}$$

with Pe the Péclet number, is approximated through its asymptotes, resulting in

$$A(Pe) \cong \max(-Pe,\ 1.0 - Pe/2.0,\ 0.0) \tag{2}$$

Received Sept. 27, 1993; revision received Dec. 20, 1993; accepted for publication Feb. 22, 1994.

*Graduate Student, Department of Mechanical Engineering.
†Professor, Department of Mechanical Engineering.
‡Associate Professor, Department of Applied Mathematics.
§Graduate Student, Department of Applied Mathematics.

Both Eqs. (1) and (2) result in upwinding at high Péclet numbers, which is inadequate in terms of accuracy in multidimensional situations due to the inherent artificial diffusion as pointed out by Pulliam.[2] Algebraic grid-aligned interpolation addresses this problem through higher order interpolation schemes, e.g., central differencing used by Peric',[3] quadratic upwinding described by Leonard and Mokhtari,[4] or other variations employed by Shyy et al.[5] With regard to physically based interpolation schemes the remedy has been the employment of the solution of a nonhomogeneous convection-diffusion equation, i.e.,

$$\frac{\partial}{\partial\xi}\left(\rho u\phi - \Gamma\frac{\partial\phi}{\partial\xi}\right) = S \tag{3}$$

in both flow-aligned and grid-aligned schemes. Examples can be found in the work of Raithby[6] and in particular control volume finite element schemes such as described by Baliga and Patankar,[7] Prakash,[8] and Schneider and Raw.[9] Furthermore, the function S not only provides the opportunity to account for multidimensional effects but also provides a velocity-pressure coupling allowing the use of nonstaggered grids. This was previously shown by Prakash[8] for flow-aligned interpolation and Thiart[10] for grid-aligned interpolation. It is the physically based analog to the methods of Baliga and Patankar[7] or Rhie and Chow,[11] which are based on central difference velocity interpolation.

Harms et al.[12] previously showed on the basis of orthogonal grids that in the context of Eq. (3) streamline-orientated interpolation with parabolic interface flux integration represents an unnecessary complication with regard to accuracy. Although physical interpolation is realistically attractive, it is at best second order when based on integration that assumes constant properties over surfaces and volumes. It is, on the other hand, computationally expensive and associated with instability as reported by Huang et al.[13] In this Note we wish to address the issue of computational expense by examining two alternatives to obtain and deal with coefficient and other exponential weighting functions arising out of the application of Eq. (3).

II. Derivation

Schneider and Raw[9] proposed to obtain an interface value in the following manner: ρu and Γ are assumed constant in the space ξ (0 to L) between two nodes and known from a previous iteration. The first derivative on the left of Eq. (3) is then discretized as an upwind difference, the second derivative as a central difference, and the source term S (at first $S_0 = S_L = S$) in any appropriate manner (e.g., a pressure gradient in the interpolation direction would follow from the adjacent nodal pressure difference and cross fluxes and other source terms from arithmetic averages of terms discretized at the two adjacent nodes[12]). For a noncentralized interface ($a = \xi/L$) and positive or negative interface velocity, the result is

$$\rho u\frac{\partial\phi}{\partial\xi} = \frac{\Gamma}{L}\left[\max(0, Pe)\frac{\phi_{aL}-\phi_0}{aL} - \max(-Pe, 0)\frac{\phi_L-\phi_{aL}}{(1-a)L}\right] \tag{4}$$

$$\Gamma\frac{\partial^2 u}{\partial\xi^2} = \Gamma\frac{a\phi_L - \phi_{aL} + (1-a)\phi_0}{a(1-a)(L^2/2)} \tag{5}$$

for $0 < a < 1$ and $Pe = \rho u_{aL}L/\Gamma$. Substituting Eqs. (4) and (5) into Eq. (3) results in

$$\phi_{aL} = \phi_0 + \frac{a}{k}[\max(-Pe, 0) + 2](\phi_L - \phi_0) + \frac{L^2}{k\Gamma}a(1-a)S \tag{6}$$

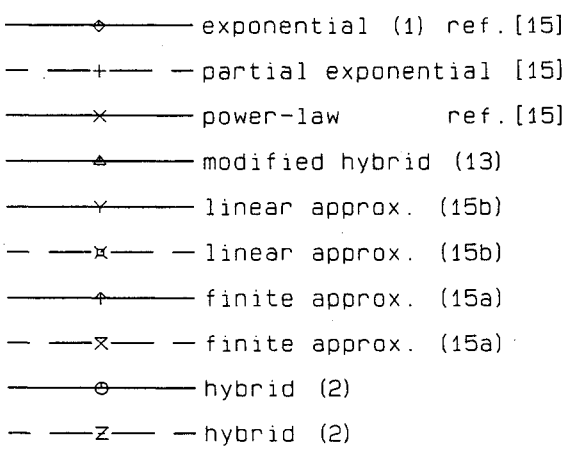

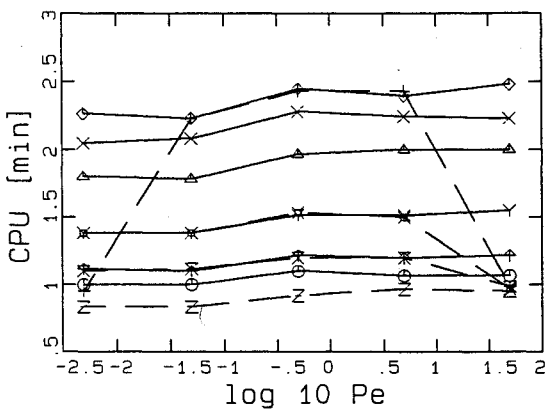

Fig. 1 Results of time trials.

where k is given by

$$k = (1-a)\max(0, Pe) + a\max(-Pe, 0) + 2 \tag{7}$$

As was shown previously,[12] and similar to the approach described by Karki et al.,[14] we can apply Eq. (7) to two regions of constant source to generate a flux spline at the control volume interface. The result is

$$\phi_{aL} = \phi_0 + C(a, Pe)\,(\phi_L - \phi_0) + \frac{L^2}{\Gamma} BD(a, -Pe)\,S_0 + \frac{L^2}{\Gamma} BD(1-a, Pe)\,S_L \tag{8}$$

with the weighting functions being

$$C(a, Pe) = a[a\max(-Pe, 0) + 2] \times [(1-a)\max(-Pe, 0) + 2]/H \tag{9}$$

$$BD(a, -Pe) = a^2(1-a)[(1-a)\max(0, Pe) + 2]/H \tag{10}$$

$$H = (1-a)[(1-a)\max(0, Pe) + 2][a\max(0, Pe) + 2] + a[(1-a)\max(-Pe, 0) + 2][a\max(-Pe, 0) + 2] \tag{11}$$

The interface convection-diffusion flux can now be assembled from previous equations[12] and expressed as

$$J_{aL} = \rho u_{aL}\phi_0 + \frac{\Gamma}{L} A(Pe)\,(\phi_0 - \phi_L) + L\,BC(a, -Pe)\,S_0 - L\,BC(1-a, Pe)\,S_L \tag{12}$$

where

$$A(Pe) = \{2[\max(0, Pe) + 4][\max(-Pe, 0) + 4] - Pe[\max(-Pe, 0) + 4]^2\}/\{[\max(0, Pe) + 4]^2 + [\max(-Pe, 0) + 4]^2\} \tag{13}$$

and

$$BC(a, -Pe) = a^2\{(1-a)\max(-Pe, 0) + 2 + (1-a)[(1-a)\max(Pe, 0) + 2]\,Pe\}/H \tag{14}$$

Analogous to previous work[12] it is now a trivial matter to extract functions B and D from Eqs. (9–11) and (14). For the sake of brevity, however, attention is rather focused on Eq. (13), noting[12] that it can be used to express the other weighting functions. Equation (13) has been optimized by letting $a = 0.5$ irrespective of the actual interface location, which follows from the homogeneous form of Eq. (3). The result is a modified hybrid approximation. It approaches the asymptotes from below, which could easily be removed by introducing additional absolute value operators.

III. Alternative Approximations

At this point two further approximations of the function $A(Pe)$ (FUNCTION APECL) are introduced as follows in terms of their Fortran 77 equivalent:

```
APECL = ANEW(INT{AMIN1[Z1, ABS (PE) ]/Z3} + 1)
  + AMAX1 (-PE, 0.0)
```

(15a)

```
I = INT{AMIN1 [Z1, ABS (PE) ] /Z3} + 1
APECL = ANEW (I) + BNEW (I) *[ABS (P)
  -REAL (I - 1) *Z3] + AMAX = 1 (-PE, 0.0)
```

(15b)

The finite approximation (15a) is based on an array (ANEW) with Z2 + 1.0 elements, in which values determined by a Fortran equivalent[15] of Eq. (1) have been deposited over the range $0 \le Pe \le Z1$ in equal increments of $Z3$, with $Z3 = Z1/Z2$. Whereas $Z1$ determines the maximum accuracy at the asymptotic jump, $Z2$ is determined accordingly to obtain the same accuracy near the origin, where $A(Pe)$ ($Pe > 0$) has a local maximum first derivative. Similarly the constant increment in the linear approximation (15b) is based on the maximum second derivative of $A(Pe)$ occurring at the origin, with BNEW being the incremental slope. In Table 1 the approximate maximum errors based on the Fortran equivalent of Eq. (1)[15] are indicated for the various approximations.

IV. Test Calculations

Time trials were executed on the University of Stellenbosch VAX 6000/410 machine using its VMS 5.5-2 operating system and the Fortran 77 version 5.8. One million calculations of the function product A·B·C·D expressed in terms of $A(Pe)$ (Ref. 12), with $a = 0.5$, were executed at five Péclet numbers in each case (0.005, 0.05, 0.5, 5, and 50). At least three runs each were executed for every data point to minimize the influence of system performance variations. The results are shown in Fig. 1, where we have also included calculations based on previous work[15] for comparison. The dashed lines indicated alternative formulations that employ Fortran IF-statements to eliminate redundant calculations at high Péclet numbers.[15] It can be seen that in terms of accuracy

Table 1 Maximum error of the approximations

Equation	Z1	Z2	Maximum error	Péclet number
(2)	2.0	——	0.313	2.0
(13)	——	——	0.236	12.9
(15a)	10.0	11,013	0.00045	10.0
(15a)	12.61	150,000	0.000042	12.61
(15b)	10.0	2×68	0.00045	10.0

the finite approximations based on Eqs. (15a) and (15b) performed best. In terms of speed it was found that no significant change resulted from employing a 150,000 element array as indicated in Table 1. In the context of the times shown in Fig. 1, the overhead to generate such an array was less than 3 s.

V. Conclusion

The derivation of the exponential-free modified hybrid approximation was motivated by the need to deal as efficiently as possible with the weighting functions arising in the physically based interpolation scheme considered. The alternative approximations, however, clearly appear to represent the most efficient option examined and, in general, can be very effective whenever a parametric dependence on a few variables arises in lengthy calculations. Their accuracies are fully adjustable at the cost of memory allocated rather than computational speed.

References

[1]Spalding, D. B., "A Novel Finite Difference Formulation for Differential Expressions Involving both First and Second Derivatives," *International Journal for Numerical Methods in Engineering*, Vol. 4, No. 4, 1972, pp. 551–559.

[2]Pulliam, T.H., "Artificial Dissipation Models for the Euler Equations," *AIAA Journal*, Vol. 24, No. 12, 1986, pp. 1931–1940.

[3]Peric′, M., "Analysis of Pressure-Velocity Coupling on Nonorthogonal Grids," *Numerical Heat Transfer*, Pt. B, Vol. 17, No. 1, 1990, pp. 63–82.

[4]Leonard, B. P., and Mokhtari, S., "Beyond First-Order Upwinding: The ULTRA-SHARP Alternative for Non-Oscillatory Steady-State Simulation of Convection," *International Journal for Numerical Methods in Engineering*, Vol. 30, No. 4, 1990, pp. 729–766.

[5]Shyy, W., Thakur, S., and Wright, J., "Second-Order Upwind and Central Difference Schemes for Recirculating Flow Computation," *AIAA Journal*, Vol. 30, No. 4, 1992, pp. 923–932.

[6]Raithby, G. D., "Skew Upstream Differencing Schemes for Problems Involving Fluid Flow," *Computer Methods in Applied Mechanics and Engineering*, Vol. 9, 1976, pp. 153–164.

[7]Baliga, B. R., and Patankar, S.V., "A Control Volume Finite-Element Method for Two-Dimensional Fluid Flow and Heat Transfer," *Numerical Heat Transfer*, Vol. 6, No. 3, 1983, pp. 245–261.

[8]Prakash, C., "An Improved Control Volume Finite-Element Method for Heat and Mass Transfer, and for Fluid Flow Using Equal-Order Velocity Pressure Interpolation," *Numerical Heat Transfer*, Vol. 9, No. 3, 1986, pp. 253–276.

[9]Schneider, G. E., and Raw, M. J., "Control Volume Finite-Element Method for Heat Transfer and Fluid Flow Using Colocated Variables - 1. Computational Procedure," *Numerical Heat Transfer*, Vol. 11, No. 4, 1987, pp. 363–390.

[10]Thiart, G. D., "Improved Finite-Difference Scheme for the Solution of Convection-Diffusion Problems with the SIMPLEN Algorithm," *Numerical Heat Transfer*, Pt. B, Vol. 18, No. 1, 1990, pp. 81–95.

[11]Rhie, C. M., and Chow, W. L., "Numerical Study of Turbulent Flow Past an Airfoil with Trailing Edge Separation," *AIAA Journal*, Vol. 21, No. 11, 1983, pp. 1525–1532.

[12]Harms, T. M., von Backström, T. W., and Du Plessis, J. P., "Reformulation of the SIMPLEN Discretization Scheme to Accommodate Noncentralized Interfaces," *Numerical Heat Transfer*, Pt. B, Vol. 20, No. 2, 1991, pp. 127–144.

[13]Huang, P. G., Launder, B. E., and Leschziner, M. A., "Discretization of Nonlinear Convection Processes: A Broad-Range Comparison of Four Schemes," *Computer Methods in Applied Mechanics and Engineering*, Vol. 48, No. 1, 1985, pp. 1–24.

[14]Karki, K. C., Patankar, S. V., and Mongia, H. C., "Three-Dimensional Fluid Flow Calculations Using a Flux-Spline Method," *AIAA Journal*, Vol. 28, No. 4, 1990, pp. 631–634.

[15]Harms, T. M., Du Plessis, J. P., and von Backström, T. W., "Derivation of a Modified Power-Law Approximation," *Numerical Heat Transfer*, Pt. B, Vol. 22, No. 2, 1992, pp. 235–241.

Approximations for Weak and Strong Oblique Shock Wave Angles

Anthony M. Agnone*

Hofstra University, Hempstead, New York 11550

Introduction

IN fluid mechanics computations, such as in the study of shock-boundary layer interactions, the oblique shock wave angle is needed as an explicit function of the upstream Mach number M and the flow turning angle δ. In Ref. 1, approximate shock-flow angle relations are developed from series expansions of the exact equation [Eq. (1) of Ref. 1]. The resulting expressions [Eqs. (13) and (14) of Ref. 1] are limited to weak oblique shocks and small wedge angles. In Ref. 2, it is commented that those approximate relations do not asymptote correctly in the limit of the infinite Mach number. Here, a simple exact explicit relation is obtained for the case of an infinite Mach number that is valid for both weak and strong shocks. Approximate relations for both weak and strong shocks are also derived for finite Mach numbers and moderate wedge angles.

Derivation of Equations

Equation 1 of Ref. 1, [or Eq. (148) of Ref. 3] can be recast into a cubic equation for the square of the sine of the shock wave angle θ as follows [see Eq. (150a) of Ref. 3]:

$$\sin^6\theta + b\sin^4\theta + c\sin^2\theta + d = 0 \tag{1a}$$

where

$$b = -(M^2+2)/M^2 - \gamma\sin^2\delta \tag{1b}$$

$$c = (2M^2+1)/M^4 + [(1/4)(\gamma+1)^2 + (\gamma-1)/M^2]\sin^2\delta \tag{1c}$$

$$d = -\cos^2\delta/M^4 \tag{1d}$$

and γ is the ratio of specific heats. Exact explicit equations for the three real roots of this cubic equation can be found in Ref. 4; however they are not easily approximated. Here simple relations are derived by noting that in the limit of infinite Mach number, the coefficient d vanishes and b and c simplify to

$$b' = -1 - \gamma\sin^2\delta \tag{2a}$$

and

$$c' = [(\gamma+1)^2/4]\sin^2\delta \tag{2b}$$

Then Eq. (1a) is reduced to a quadratic and its two roots can be obtained from

$$\sin^2\theta_\infty = (1/2)[-b' \pm (b'^2 - 4c')^{1/2}] \qquad \text{for } M_\infty \to \infty \tag{3}$$

The positive and negative signs correspond to the strong and weak shock, respectively. This equation is represented graphically in Fig. 1 for $\gamma = 1.4$ and is compared with $\theta \approx (\gamma+1)\delta/2$, [Eq. (3a) of Ref. 5]. As shown in Fig. 1, the latter is accurate for $\delta < 25$ deg. The disappearance of the third but physically inadmissible root is evident from the shock polar in that the limit circle (for $M = \infty$) coincides with the approach flow circle.

Approximate but accurate relations for finite Mach numbers are obtained by noting that d is small since it depends inversely on the

Received Oct. 4, 1993; revision received Feb. 23, 1994; accepted for publication March 5, 1994.

*Associate Professor, Department of Engineering. Senior Member AIAA.